Cylindrical Cell Model for the Hydrodynamics of Particle Assemblages at Intermediate Reynolds Numbers

REUVEN TAL (THAU) and W. A. SIRIGNANO

Department of Mechanical Engineering
Carnegie-Mellon University
Pittsburgh, PA 15213

The spherical cell model for transport in assemblages of spheres, which stems from the low Reynolds number hydrodynamics, has a serious physical limitation when extended to the range of intermediate Reynolds numbers. Spherical symmetry cannot persist around a sphere, given a definite direction of convection. The boundary conditions of the spherical cell model are inappropriate and a cubic cell model would best represent the system. However, in order to avoid undue mathematical difficulties peculiar to three-dimensional problems, a cylindrical cell model is proposed.

A numerical solution of the Navier-Stokes equations expressed in vorticity-stream function variables has been performed in conjunction with the cylindrical cell model for various values of porosity and Reynolds number. A much better agreement of the drag coefficient with experimental results is obtained by the cylindrical cell model than by the spherical cell model.

SCOPE

The objective of the study was to develop a physically-sound theoretical hydrodynamic model for assemblages of spheres at intermediate Reynolds numbers in order to calculate the flow field with satisfactory accuracy. Previously proposed theoretical cell models, developed for low Reynolds numbers and extended without major modifications to intermediate Reynolds numbers, lack the above mentioned features. The assumption of a cell with spherically-symmetric zero stress or zero vorticity boundary conditions is especially artificial at intermediate Reynolds numbers, where convective effects become important. The limitation of existing cell models for intermediate Reynolds numbers was first indicated by LeClair and Hamielec (1968) but since that time no significant improvement has been proposed.

The genesis of the present work is in the study of interaction of vaporizing fuel droplets which are injected into a combustor at Re $\cong$ 100. In addition, there is a great variety of systems including packed beds and fludized beds where interactions between the dispersed elements are important and need a sound theoretical basis.

CONCLUSIONS AND SIGNIFICANCE

A clyindrical cell model for transport in assemblages of spheres at intermediate Reynolds numbers has been developed. The model is not limited to intermediate Reynolds numbers and we believe it is physically sounder than the spherical cell model even at Re $\ll$ 1. However, due to our interest in spray vaporization in a combustor we addressed first the range of intermediate Reynolds numbers.

Probably due to its more plausible physical formulation, the cylindrical cell model predicts drag coefficients with much better accuracy than previous models did.

Interacting spheres, as compared to a single sphere, feature a higher drag coefficient, a thinner boundary layer and a shrunk recirculating zone. Interactions are quantitatively most significant for an average distance between the spheres of less than two diameters and are practically negligible for an average distance between the spheres of more than 5 diameters.

The present work is the basis for calculating heat and mass transfer (and ultimately vaporization rates) for a spray of hydrocarbon fuel droplets. The continuous phase analysis will be coupled with the disperse (i.e., liquid) phase solution developed by Prakash and Sirignano (1978, 1980) and Lara-Urbaneja and Sirignano (1980). The model can also be applied for transport phenomena in fludized and packed beds. Rheological properties of suspensions will also be considered in the future.

LOW REYNOLDS NUMBERS HYDRODYNAMICS: ORIGIN OF SPHERICAL CELL MODEL

Despite the many practical systems involving assemblages of bubbles, drops or particles dispersed in a continuous phase, there is basically only one model to describe the mutual interactions in such systems: the spherical cell model, due to Happel (1958) and Kuwabara (1959). In its formulation, the complex multi-particle problem is replaced by a conceptually simple and mathematically attractive one involving only one particle surrounded by a fluid envelope containing a volume of fluid sufficient to make the fractional void volume in the cell identical to that in the entire assemblage. [At the outside surface of each cell zero stress was assumed by Happel (1958) and zero vorticity by Kuwabara (1959).] Thus the entire influence of each particle is confined to the cell of fluid with which it is associated. It should be stressed that the spherical cell model was developed for the domain of low Reynolds numbers, where the viscous effects are dominant compared to convective effects. In this domain, the model predicted successfully the pressure drop for packed beds in the range of voidages $0.3 \leq \epsilon \leq 0.6$. The Happel solution for solid particles has been generalized by Gal-Or and Waslo (1968) to include swarms of drops and bubbles in the presence (or absence) of surfactant impurities. Yaron and Gal-Or (1971) used the hydrodynamic solution of Gal-Or and

0001-1541-82-5242-0233-$2.00.

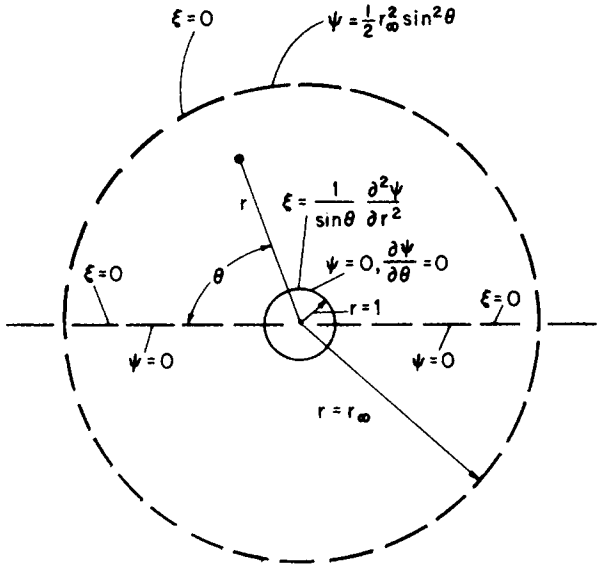

Figure 1. Spherical cell model boundary conditions.

Waslo (1968) to calculate heat and mass transfer from side distributed drops, bubbles or solid particles and later the effective viscosity of concentrated suspensions and emulsions (1972).

It is fair to mention the doubts about the physical justification of the spherical cell model from the very beginning. Happel and Brenner (1973) state that the spherical shape was assumed for simplicity. Brenner (1957) tried to solve the more meaningful problem of a sphere in a cubical cell of fluid, trying to satisfy the boundary conditions on the sphere and at individual selected points on the cubic envelope. Numerical solution of the resulting set of simultaneous equations for this three dimensional problem proved intractable. The idealization in the spherical cell assumption was also indicated by Gal-Or (1970).

EXTENSION OF SPHERICAL CELL MODEL TO INTERMEDIATE REYNOLDS NUMBERS

LeClair and Hamielec (1968) extended the spherical cell model developed by Happel (1958) to the range of intermediate Reynolds numbers. The complete Navier-Stokes equation was solved for axisymmetric flows around spherical particles in an assemblage. The geometry of the model is presented in Figure 1. The boundary conditions used by LeClair and Hamielec (1968) are:
Along the axis of symmetry:

$$\theta = 0^\circ \text{ and } \theta = 180^\circ, \psi = 0, \xi = 0 \tag{1}$$

on the sphere surface:

$$r = 1, \psi = 0, \frac{\partial \psi}{\partial r} = 0 \text{ and } \xi = \frac{E^2\psi}{\sin\theta} \tag{2}$$

where

$$E^2 \equiv \frac{\partial^2}{\partial r^2} + \frac{\sin\theta}{r^2}\frac{\partial}{\partial\theta}\left(\frac{1}{\sin\theta}\frac{\partial}{\partial\theta}\right) \tag{3}$$

On the outer boundary

$$r = r_\infty, \xi = 0, \psi = \tfrac{1}{2}r_\infty^2 \sin^2\theta \tag{4}$$

(uniform flow)
the porosity of the sphere assemblage being:

$$\epsilon = 1 - r_\infty^{-3} \tag{5}$$

The solution of LeClair and Hamielec shows some very interesting features of the hydrodynamics of sphere assemblages at intermediate Reynolds numbers:

a) The effect of reduction in porosity is to reduce the dimensions of the recirculating zone, i.e., to increase the angle of separation and decrease the length of the recirculating zone.
b) The maximum velocity increases as the porosity decreases. The boundary layer thickness decreases with decreasing of the porosity.

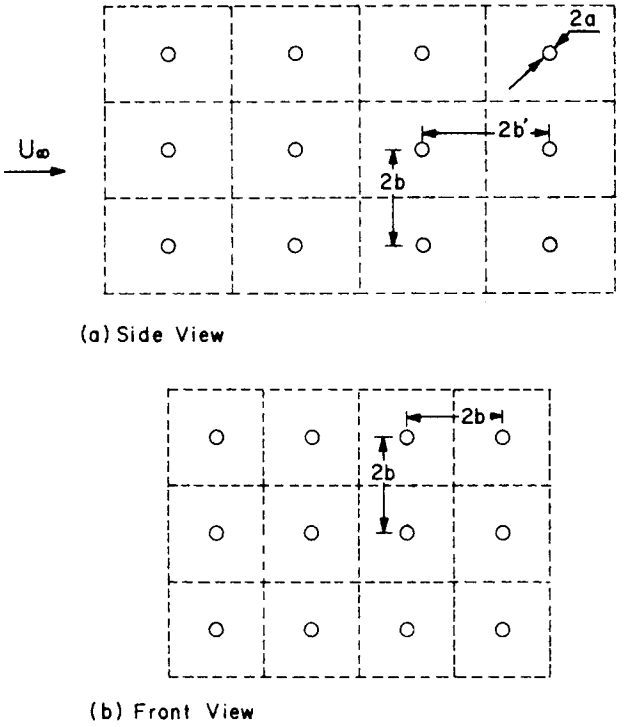

Figure 2. Geometrical representation of an array of spheres.

LeClair and Hamielec (1968) obtained good agreement with experimental drag coefficient results only up to Re = 30. In explaining the reasons for the drag discrepancy at higher Reynolds number, LeClair and Hamielec state that the model developed by Happel does not truly represent the local flow behavior in multiparticle systems; however, it is easy to apply. To improve the results, they suggest the determination of boundary conditions on the outer boundary which may more truly represent the actual local flow behavior. One of their suggestions is using prolate or oblate spheroids (depending on the Reynolds number) instead of spheres as cell boundaries. Based upon this suggestion, El-Kaissy and Homsy (1973) developed a distorted cell model and parametrically selected the cell shape for every specific Reynolds number to fit the experimental drag data. As El-Kaissy and Homsy (1973) state, this is a serious loss of generality; however, fitting of the cell shape can be useful for specific heat and mass transfer applications. In principle, it is hard to accept a model with boundary shape and conditions dependent upon the Reynolds number.

CYLINDRICAL CELL MODEL

Looking at the geometrical representation of an idealized rectangular array of spheres (being of the same size and equidistant) (Figure 2), it becomes apparent that the equidistant planes between the spheres create rectangular cells. The boundaries of these cells have properties of symmetry and periodicity; however, there is considerable difficulty in solving the non-axisymmetric, three-dimensional problem posed by the flow around a sphere in a rectangular cell. For that reason, a cylindrical cell is proposed with a void fraction equivalent to that of the rectangular cell. The radius of the cylindrical cell is $b\sqrt{4/\pi}$ and its length $2b'$ (Figure 2). In the following, we assume $b = b'$ and consider a cubic cell.

The porosity is related to the array geometry by the following equation

$$\epsilon = 1 - \frac{\pi}{6}\left(\frac{b}{a}\right)^{-3} \tag{6}$$

The incompressible Navier-Stokes equations in spherical coordinates expressed in vorticity-stream function variables are:

$$\frac{\mathrm{Re}\sin\theta}{2}\left[\frac{\partial\psi}{\partial r}\frac{\partial}{\partial\theta}\left(\frac{\xi}{r\sin\theta}\right)-\frac{\partial\psi}{\partial\theta}\frac{\partial}{\partial r}\left(\frac{\xi}{r\sin\theta}\right)\right]=E^2(\xi r\sin\theta) \quad (7)$$

$$E^2\psi=\xi r\sin\theta \quad (8)$$

The velocity components are being expressed as:

$$V_\theta=\frac{1}{r\sin\theta}\frac{\partial\psi}{\partial r} \quad (9)$$

$$V_r=-\frac{1}{r^2\sin\theta}\frac{\partial\psi}{\partial\theta} \quad (10)$$

all quantities have been made dimensionless by putting:

$$r=\frac{r^*}{a},\ \psi=\frac{\psi^*}{V_\infty a^2},\ \xi=\frac{\xi^* a}{V_\infty},\ V_r=\frac{V_r^*}{V_\infty},\ V_\theta=\frac{V_\theta^*}{V_\infty} \quad (11)$$

The boundary conditions for the cylindrical cell model are: Along the axis of symmetry:

$$\theta=0^\circ \text{ and } \theta=180^\circ:\psi=0,\ \xi=0 \quad (12)$$

On the sphere:

$$r=1:\psi=0,\ \frac{\partial\psi}{\partial r}=0 \text{ and } \xi=\frac{E^2\psi}{\sin\theta} \quad (13)$$

On the cylindrical envelope ($r\sin\theta=\rho_{\max}$):

$$\rho_{\max}=\frac{b}{a}\sqrt{\frac{4}{\pi}} \quad (14)$$

$$\psi=\frac{1}{2}(r^2\sin^2\theta)|_{r\sin\theta=\rho_{\max}}=\frac{1}{2}\rho_{\max}^2 \quad (15)$$

$$\xi=0 \quad (16)$$

On the bases of the cylindrical cell [$x=\pm(b/a)$]

$$\frac{\partial\psi}{\partial x}=0 \quad (17)$$

$$\frac{\partial\xi}{\partial x}=0 \quad (18)$$

The cylindrical polar coordinate are defined as:

$$x=r\cos\theta \quad (19)$$

$$\rho=r\sin\theta \quad (20)$$

As the stream function and vorticity are expected to vary most rapidly near the surface of the sphere, it is desirable to define a new radial coordinate having the property of fine grid spacing near the sphere surface while becoming coarser in regions far removed from the surface. A convenient transformation, first used by Jenson (1959) is:

$$r=e^z \quad (21)$$

Equations 7 and 8 become:

$$E^2(\xi e^z\sin\theta)-\frac{\mathrm{Re}\sin\theta}{2e^z}\left[\left(\frac{\partial\psi}{\partial z}\right)\frac{\partial}{\partial\theta}\left(\frac{\xi}{e^z\sin\theta}\right)-\left(\frac{\partial\psi}{\partial\theta}\right)\frac{\partial}{\partial z}\left(\frac{\xi}{e^z\sin\theta}\right)\right]=0 \quad (22)$$

$$E^2\psi-\xi e^z\sin\theta=0 \quad (23)$$

where

$$E^2\equiv\frac{1}{e^{2z}}\left[\frac{\partial^2}{\partial z^2}-\frac{\partial}{\partial z}+\sin\theta\frac{\partial}{\partial\theta}\left(\frac{1}{\sin\theta}\frac{\partial}{\partial\theta}\right)\right] \quad (24)$$

The boundary conditions 12–18 previously written in $r-\theta$ coordinates are transformed into $z-\theta$ coordinates:
Along the axis of symmetry:

$$\theta=0^\circ,\ \theta=180^\circ:\psi=0,\ \xi=0 \quad (25)$$

On the sphere ($z=0$):

$$\psi=0,\ \frac{\partial\psi}{\partial z}=0,\ \xi=\frac{1}{\sin\theta}\frac{\partial^2\psi}{\partial z^2} \quad (26)$$

On the envelope of the cylinder, for corresponding values of θ:

$$\arctan\sqrt{\frac{4}{\pi}}\le\theta\le\pi-\arctan\sqrt{\frac{4}{\pi}}$$

$$\text{for } z_M(\theta)=\ln\left(\frac{\frac{b}{a}\sqrt{\frac{4}{\pi}}}{\sin\theta}\right)$$

$$\xi=0 \quad (27)$$

$$\psi=\frac{2}{\pi}\left(\frac{b}{a}\right)^2 \quad (28)$$

On the bases of the cylinder, for the corresponding values of θ:

$$\theta<\arctan\sqrt{\frac{4}{\pi}} \text{ or } \theta>\pi-\arctan\sqrt{\frac{4}{\pi}}$$

$$\text{for } z_m(\theta)=\ln\left(\frac{\frac{b}{a}}{\cos\theta}\right)$$

$$\frac{\partial\psi}{\partial x}=0,\ \frac{\partial\xi}{\partial x}=0 \quad (29)$$

The derivative $\partial/\partial x$ is calculated by the chain rule:

$$\frac{\partial}{\partial x}=\frac{\partial z}{\partial x}\frac{\partial}{\partial z}+\frac{\partial\theta}{\partial x}\frac{\partial}{\partial\theta} \quad (30)$$

The conversion procedure of the two partial differential Eqs. 22, 23 to a second-order accurate finite-difference form followed the scheme developed by Rhodes (1967) and due to its length is not reproduced here. A step size of $\Delta z=0.05$ and $\Delta\theta=6^\circ$ was used. CPU time was typically 3 minutes on a DEC-20 system for a convergence of less than 0.1% of the vorticity and stream function, using a successive over relaxation technique with uniform relaxation factors. Decreasing step size to $\Delta z=0.025$ and $\Delta\theta=3^\circ$ changes the drag coefficient by 0.3% but significantly increases CPU time.

RESULTS OBTAINED WITH CYLINDRICAL CELL MODEL

The velocity profiles at $\theta=\pi/2$ for various values of the porosity at Re = 20 are plotted in Figure 3, compared to the results of LeClair and Hamielec (1968). It is evident from this figure that the cylindrical cell model is a more severe interaction model, giving a higher peak velocity, a higher velocity derivative and a thinner boundary layer. (The basic trend of decrease in boundary layer thickness with decreasing the porosity, as described by LeClair and Hamielec (1968) still remains valid.] For that reason the cylindrical cell interaction model gives higher values of the drag coefficient as compared to the spherical cell model and therefore a better compliance with the experimental results of Ergun (1952). The improvement in the drag estimate is especially meaningful at low b/a values (Figure 4), where the interactions between neighboring spheres are the strongest. At Re = 40 and $b/a=1.4$, the cylindrical cell model estimates the drag coefficient with an accuracy of 7%, compared to 30% of the spherical cell mode. For Re = 100 and $b/a=1.4$, the cylindircal and spherical cell models estimate the drag with an accuracy of 9% and 40%, respectively. (The comparison is based on equal porosity; for convenience the abscissa is given in b/a units based on Eq. 6.)

The values of the separation angle and the length of the aft recirculation zone as functions of b/a are given in Figure 5, for Re = 100. Again, the basic trend predicted by LeClair and Hamielec (1968) (reduction in the dimension of the recirculating zone with decreasing porosity) remains valid. There is no separation at Re = 100 for b/a less than 2 and, at $b/a=4.5$, the values of the separation angle and recirculating zone length are quite close to the values for the case of uniform flow around a single sphere as reported by Taneda (1956).

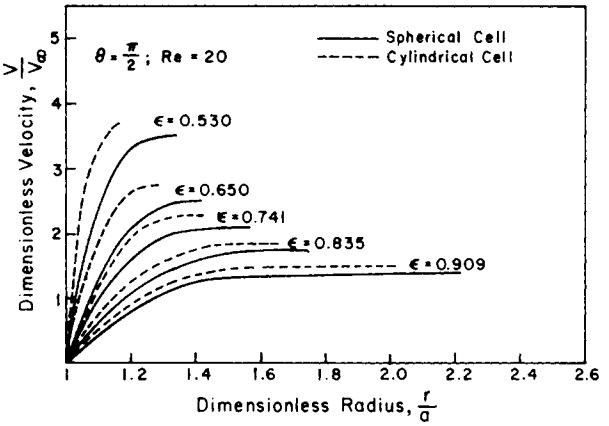

Figure 3. Velocity distribution for various porosities.

DISCUSSION

The cylindrical cell model seems to provide significant improvement in the calculated results when compared with the previously-employed spherical model. Some idealization is still present in the cylindrical model but deviations from experimental results are now within the tolerable range. It is noteworthy here that the upstream and downstream boundary conditions seem to prevent the recirculation zone aft of the sphere from crossing the cell boundary; instead the recirculation zone shrinks in size as the cell size shrinks. On the other hand, intuition would lead one to believe that for sufficiently small b/a, the recirculation zone aft of one sphere would contact the next sphere in its wake. Very likely improved boundary conditions would allow this to occur.

One cannot overemphasize the importance of the cell boundary conditions, in addition to the cell shape. Unfortunately, there is no clear-cut procedure in establishing boundary conditions for the Navier-Stokes equations even for the relatively simple problem of uniform flow around a single sphere (Rimon and Cheng, 1969). As Roache (1972) states, determining the boundary conditions relies upon intuition, wind tunnel experience and computational experimentation. It is therefore conceivable that by using the spherical cell model with boundary conditions more sophisticated than the assumption of uniform parallel flow and zero vorticity at the cell boundaries, better results could be obtained. However, besides the mere agreement between results obtained experimentally and by computational fluid dynamics, the physical bases of the various models should be considered. The cylindrical cell model, besides its quantitative computational advantages, distinguishes between the streamwise and cross-stream directions in formulating the problem. The spherical cell model lacks such a distinction.

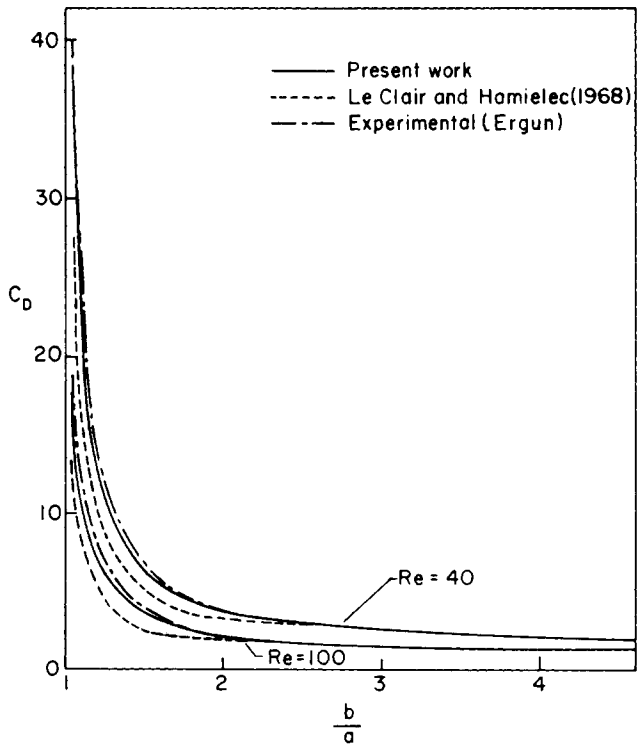

Figure 4. Drag coefficient versus porosity.

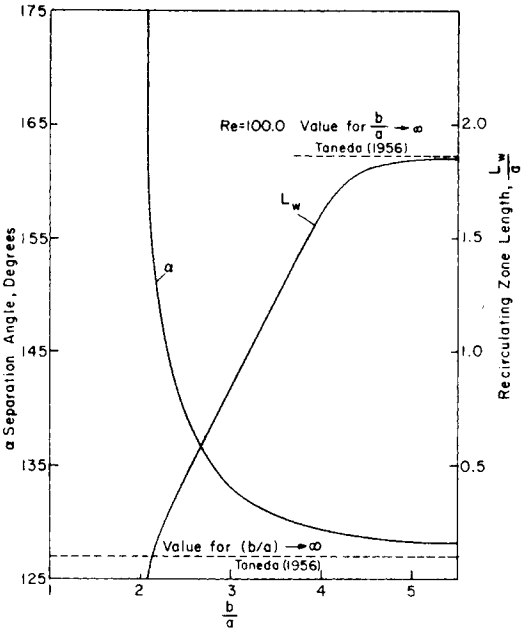

Figure 5. Vortex length and separation angle versus porosity.

The present work is only the very beginning of a large spectrum of applications for the cylindrical cell model. Some of the examples for further applications include:

(a) Hydrodynamics and coupled heat and mass transfer in assemblages of vaporizing fuel droplets in hot air.

(b) Estimating the rheological properties of suspensions.

NOTATION

a = radius of sphere in array of spheres
b = half distance between spheres in cubic array
C_D = drag coefficient
Re = Reynolds number $\frac{2aV_\infty}{\nu}$
r = radius in spherical coordinates
r_∞ = radius of spherical cell
V_∞ = approach velocity
V_r = radial velocity component
$V_{//}$ = angular velocity component
x = polar cylindrical coordinate, parallel to V_∞
z = transformed spherical coordinate
$z_M(\theta)$ = cylindrical cell boundary

Greek Letters

ξ = vorticity
θ = angular spherical polar coordinate
ψ = stream function
ρ = radius in cylindrical polar coordinates
μ = viscosity
ν = kinematic viscosity
ϵ = porosity

Subscripts and Superscripts

( )* = dimensional variable
( )$_{sep}$ = separation

LITERATURE CITED

Brenner, H., "A Theoretical Study of Slow, Viscous Flow Through Assemblages of Spherical Particles," Eng. Sc.D. Thesis, New York University, New York (1957).

El-Kaissy, M. M. and G. M. Homsy, "A Theoretical Study of Pressure Drop and Transport in Packed Beds at Intermediate Reynolds Numbers," *IEC Fund.*, **12**, 82 (1973).

Ergun, S., "Fluid Flow Through Packed Columns," *Chem. Eng. Prog.*, **48**, 89 (1952).

Gal-Or, B. and S. Waslo, "Hydrodynamics of an Ensemble of Drops (or Bubbles) in the Presence or Absence of Surfactants," *Chem. Eng. Sci.*, **23**, 1431 (1968).

Gal-Or, B., "On Motion of Bubbles and Drops," *Can. J. Chem. Eng.*, **48**, 526 (1970).

Happel, J., "Viscous Flow in Multiparticle Systems: Slow Motion of Fluids Relative to Beds of Spherical Particles," *AIChE J.*, **4**, 197 (1958).

Happel, J. and H. Brenner, *Low Reynolds Number Hydrodynamics*, Noordhoff International Publishing, Leyden, Holland (1973).

Jenson, V. G., "Viscous Flow Round a Sphere at Low Reynolds Numbers (<40)," *Proc. Roy. Soc. London*, **249A**, 346 (1959).

Kuwabara, S., "The Forces Experienced by Randomly Distributed Parallel Circular Cylinders or Spheres in a Viscous Flow at Small Reynolds Numbers," *J. Phys. Soc. (Japan)*, **14**, 527 (1959).

LeClair, B. P., and A. E. Hamielec, "Viscous Flow Through Particle Assemblages at Intermediate Reynolds Numbers," *IEC Fund.*, **7**, 542 (1968).

Lara-Urbaneja, P. and W. A. Sirignano, "Theory of Transient Multicomponent Droplet Vaporization in a Convective Field," *Proc. of the 19th Symposium (International) on Combustion*, Combustion Institute (1981).

Prakash, S. and W. A. Sirignano, "Liquid Fuel Droplet Heating with Internal Circulation, *Int. J. Heat Mass Transfer*, **21**, 885 (1978).

Prakash, S. and W. A. Sirignano, "Theory of Convective Droplet Vaporization with Unsteady Heat Transfer in the Circulating Liquid Phase," *Int. J. Heat Mass Transfer*, **23**, 253 (1980).

Rhodes, J. M., "Local Rates of Mass Transfer from Spheres in Simple Cubic Packing and a Numerical Solution of the Navier-Stokes Equations for Viscous Flow Past a Single Sphere," Ph.D. Thesis, University of Tennessee, Knoxville, TN (1967).

Rimon, Y. and S. I. Cheng, "Numerical Solution of a Uniform Flow Over a Sphere at Intermediate Reynolds Numbers," *Phys. Fluids*, **12**, 1949 (1969).

Roache, P. J., *Computational Fluid Dynamics*, Hermosa Publishing, Albuquerque, NM (1972).

Taneda, S., "Experimental Investigation of the Wake Behind a Sphere at Low Reynolds Numbers," Rept. Res. Inst. Appl. Mech., Kyushu University, **4**, 99 (1956).

Yaron, I. and B. Gal-Or "Convective Mass or Heat Transfer from Size-Distributed Drops, Bubbles or Solid Particles," *Int. J. Heat Mass Transfer*, **14**, 727 (1971).

Yaron, I. and B. Gal-Or "On Viscous Flow and Effective Viscosity of Concentrated Suspensions and Emulsions," *Rheol. Acta*, **11**, 241 (1972).

Manuscript received January 5, 1981; revision received April 17, and accepted May 6, 1981

Kinetics of High-Temperature Carbon Gasification Reaction

A simple technique is developed and is used to measure simultaneously the overall rate and the depth of the reaction zone in the porous solid. It is shown that by using some simple models, one may calculate the intrinsic rate constant and the pore diffusivity from the overall rate and the penetration depth. Models which allow for a varying pore diffusivity according to a linear porosity profile are presented, and have been shown more satisfactory than the constant diffusivity models of Thiele and of Zeldovich when applied to the high temperature carbon-carbon dioxide reaction.

N. J. DESAI and R. T. YANG

Department of Chemical Engineering
State University of New York at Buffalo
Amherst, NY 14620

SCOPE

For solid-catalyzed and most of gas-solid reactions in a porous solid, the overall reaction rate is determined by the pore diffusion rate and the chemical reaction rate. When the chemical rate is sufficiently lower than the pore diffusion rate, there is no significant concentration drop within the solid and the entire solid particle is efficiently used. On the other hand, when pore diffusion is relatively slow, the reaction is limited to within a zone on the exterior surface, which we shall call penetration depth. Many rigorous theoretical and experimental results have been published for the former case. Some of the models, such as the early ones by Thiele and by Zeldovich, may be extended to describe the kinetics for the latter case.

Most of the gas-carbon reactions under commercial conditions (i.e., at high temperatures) belong to the diffusion-controlled regime. To study the kinetics in this regime, it is much easier to measure the overall rate and the penetration depth, rather than measuring the chemical rate and the pore diffusion rate. Knowing the overall rate and the penetration depth, one may obtain information on the chemical rate and pore diffusion rate through modeling. Much experimental work has been done on measuring the penetration depth of gas-carbon reactions in the high temperature range, primarily by Golovina et al., for the C-CO_2 reaction at temperatures up to 3400 K.

In this work, a simpler and more accurate technique is developed to measure the penetration depth, which also provides data for the overall rate simultaneously. We also present kinetic models which allow for porosity and surface area variations, and hence the diffusivity variation, within the reaction zone.

Correspondence concerning this paper should be addressed to R. T. Yang.

0001-1541-82-5241-0237-$2.00